

## Director Structure in a Chiral Nematic Slab: Threshold Field and Pitch Variations

S. Shoarinejad<sup>a,\*</sup> and M.A. Shahzamanian<sup>b</sup>

<sup>a</sup>*Department of Physics, Faculty of Science, Alzahra University, Tehran, Iran*

<sup>b</sup>*Department of Physics, Faculty of Science, Isfahan University, Isfahan, Iran*

*(Received 15 May 2013, Accepted 12 August 2013)*

The liquid crystal director distribution is determined for a confined chiral nematic slab. The molecular director distribution of the field-controlled chiral nematic slab is directly calculated. The director profiles for the tilt and the twist angles, under different applied fields, are calculated in the slab with weak boundary conditions. Then, the dependence of the threshold field on a dimensionless parameter containing the anchoring and thickness variations is discussed. The variation of the threshold field is found as a function of anchoring strengths for different ratios of the slab-thickness to the pitch,  $d/P$ . It confirms that for a constant ratio of  $d/P$ , the field decreasing rate in strong anchoring conditions is high and that by decreasing the strength of anchoring, the threshold field becomes approximately constant. This study is based on a stable and simple numerical method that gives accurate results in a short time, compared to the existing methods and a good agreement with the previously reported solutions highlights the effectiveness of the method.

**Keywords:** Threshold field, Chiral Twisted Nematic, Anchoring, Pitch variations

### INTRODUCTION

A nematic liquid crystal is a phase of liquid crystals with the least order and the highest symmetry. It solely exhibits the orientation of the long molecular axis, *i.e.*, the director  $\mathbf{n}$  as a globally preferred direction. The deformations of a nematic liquid crystal due to the external forces, such as boundary forces, electric or magnetic fields increase the free energy density as compared to a uniformly aligned nematic. This increase in energy is described by the continuum theory that first proposed by Oseen and developed by Frank [1]. All bulk deformations of a nematic phase can be traced back to three fundamental elastic deformations called splay, twist and bend [2-4].

Similarly, the chiral nematic liquid crystal phase solely possesses the orientation of the long molecular axis. However, in contrast to the nematic phase, there is a spontaneous macroscopic helical superstructure with a twist axis perpendicular to the local director. Thus the phase consists of local nematic layers, which are continuously twisted with respect to each other. Hence, chiral nematic

phases exhibit an inherent twist with the twist axis perpendicular to the local director and a pitch  $P$  of the undisturbed helix. This is accounted for in the expression of the free energy density by inclusion of the helical wave vector  $q_0 = 2\pi/p$ , called free twist number or twisting number [3-6]. The distortions induced by external fields applied to chiral nematic liquid crystal give rise to a wide range of magneto-optic and electro-optic effects. There is strong interest in novel and improved liquid crystal technologies through magnetically, electrically, and optically induced Fredericks transitions [7]. Fredericks transition refers to reorientation of the director induced by magnetic or electric fields [8]. These phenomena have been the subject of extensive studies during the last few decades [9-11]. However, despite prior studies, many features are yet to be systematically investigated.

The magneto-optical and electro-optical properties depend on the alignment angle of the director at the surface (pretilt angle) imposed by the substrate boundaries as well as the bulk material properties. In chiral nematic liquid crystals, the surface anchoring effects and the external fields are important both for basic understanding of the theory as well as in a wide range of applications. In principle, the

\*Corresponding author. E-mail: [sshoari@alzahra.ac.ir](mailto:sshoari@alzahra.ac.ir)

interfacial free energy, called anchoring energy, has been introduced in order to quantify how strongly a nematic liquid crystal is oriented or anchored [3-5]. In most cases of twisted chiral nematic liquid crystals, the surface coupling is not so strong and hence the concept of weak anchoring has been introduced. To describe a weak anchoring surface for an untwisted nematic liquid crystal sample, Rapini and Papoular have introduced a simple expression for the interfacial energy per unit area for a one dimensional deformation [12]

For the two dimensional deformation cases, such as a twisted nematic liquid crystal cell, a general anchoring energy expression is necessary [13]:

$$f_s = \frac{W_{ij}}{2} [1 - (n \cdot e)^2] \tag{1}$$

which  $W_{ij}$  is a nonlinear combination of the azimuthal and the polar angles. In this expression,  $e$  is the easy direction of the boundary surfaces and  $W_{ij}$  represents the anchoring strengths.

It is well known that the magneto-optical and electro-optical properties of twisted devices are modified by altering the director field. Thus determining the behavior of the director field is critical. In this article, the molecular director distribution of the field-controlled twisted chiral nematic slab is directly calculated. It is assumed that the two limiting planes of the slab are treated in a way that leads to the surface interaction imposing a specified orientation  $e$  on the liquid crystal, and that they are in weak anchoring conditions. A stable, simple and fast method which is based on a finite difference approximation is used [8]. The dependence of the director distribution and the threshold field on deformation, anchoring strength and the confinement ratio is studied under certain magnetic fields. The confinement ratio is defined as the ratio of the slab-thickness to the pitch,  $d/P$ . It is shown to provide accurate results in line with the previously reported results [14].

### PROBLEM FORMULATION

We are concerned with the orientational structures in a chiral nematic slab bounded by two parallel planes. In such slabs, director distributions are strongly affected by the anchoring conditions at the boundary surfaces which break the translational symmetry along the twisting axis. In

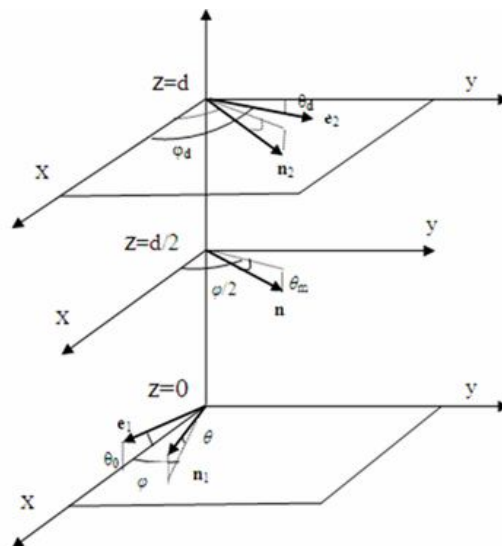


Fig. 1. Polar and azimuthal variables with respect to the director.

addition, there is a magnetic field applied to the slab. So, in general, all the factors (chirality, elasticity, magnetic torques and surface anchoring) are in direct competition and the helical form of the director field will be distorted. To formulate such a complex problem we consider a twisted chiral nematic slab of thickness  $d$  with two parallel planes at  $z = 0$  and  $z = d$ . It is subjected to finite anchoring at these surfaces as shown in Fig. 1. In practice, finite anchoring means that the extrapolation length not be small compared with both the slab thickness and the magnetic coherence length. A magnetic field, parallel to the  $z$  axis, is then applied between the boundary planes. On one hand, it is enforced by anchoring forces at the confining surfaces and the chirality. On the other hand, the magnetic field exerts a torque which may conflict with the chirality and boundary-imposed alignment. The torque increases with an increase in the field strength, and tends to reorient the layers along the field, but free rotations are hindered by limiting surfaces. It is shown that eventually, at certain field strength, the boundary-imposed alignment becomes unstable and gets replaced by the imposed field ultimately affecting the director distribution. A large variety of nonlinear phenomena occurs as a result of this feedback. For a confined chiral nematic liquid crystal, the nonlinear phenomena can be formulated as presented in this section.

The elastic free energy density in the bulk of a chiral nematic liquid crystal can be explained in terms of the Oseen-Frank strain free energy density:

$$f_{el} = \frac{1}{2} \{k_{11}(\nabla \cdot n)^2 + k_{22}(n \cdot \nabla \times n + q_0)^2 + k_{33}[n \times (\nabla \times n)]^2\} \quad (2)$$

where  $K_{11}, K_{22}, K_{33}$  are the elastic coefficients, for splay, twist, and bend, respectively, and  $q_0$  gives the equilibrium helical pitch  $p_0 = 2\pi/q_0$  for the twist axis directed along  $z$  direction. Then, the equilibrium configuration in an unbounded chiral nematic liquid crystal is defined by the director field:  $\mathbf{n} = (\cos q_0 z, \sin q_0 z, 0)$ . When the chiral nematic liquid crystal is bounded with planar anchoring condition, it might be expected that the helix twist wave number differ from  $q_0$  [11].

The orientation of the director of the bounded chiral nematic slab may be described by two angles,  $\theta$  (the tilt angle measured from the surface  $x$ - $y$ ) and  $\varphi$  (the twist angle corresponding to the spherical coordinate), Fig. 1:

$$n = (\cos \theta \cos \varphi, \cos \theta \sin \varphi, \sin \theta) \quad (3)$$

It is assumed that the configurations are stable with respect to out of plane director fluctuations and the distortions depend on twisting number and one dimension,  $z$ . The magnetic free energy density is given by:

$$f_{field} = \mu_0^{-1} (x_{\perp} B^2 + x_{\alpha} (n \cdot B)^2) \quad (4)$$

where  $x_{\alpha}$  is the magnetic susceptibility anisotropy, *i.e.*, the difference between the susceptibilities parallel and perpendicular to the local director. The more general form of surface energy, Eq. (1), is used for anchoring energies of the boundary planes at  $z = 0$  and  $z = d$ . The easy direction  $e$  of the boundary surfaces can be written as:

$$e = (\cos \theta \cos \phi, \cos \theta \sin \phi, \sin \theta) \quad (5)$$

where  $\theta$  and  $\phi$  are the tilt and the azimuthal angles of the director at the easy direction, respectively. Corresponding surface energy densities for the bottom and the top planes are given by:

$$f_s^1 = \frac{W_1}{2} [1 - (n_1 \cdot e_1)^2] \quad \text{for } z = 0 \quad (6)$$

$$f_s^2 = \frac{W_2}{2} [1 - (n_2 \cdot e_2)^2] \quad \text{for } z = d \quad (7)$$

where  $W_{2,1}$  are the anchoring strengths at the top and the bottom planes. The easy directions may be expressed as the following unit vectors:

$$e_1 = (\cos \theta_0, 0, \sin \theta_0) \quad \text{for } z = 0 \quad (8)$$

$$e_2 = (\cos \theta_d \cos \varphi_d, \cos \theta_d \sin \varphi_d, \sin \theta_d) \quad \text{for } z = d \quad (9)$$

where  $\theta_{0,d}$  and  $\varphi_{0,d}$  are the boundary values of the orientation angles of the director, as shown in Fig. 1. Accordingly, the total free energy including the bulk energy and the surface free energies is obtained by:

$$F = \int_{slab} (f_{el} + f_{chiral} + f_{field}) dV + \int_{s1} f_s^1 ds + \int_{s2} f_s^2 ds \quad (10)$$

where  $dV$  is the volume element of the bulk energy,  $ds$  is the surface area element of the bottom and the top planes. The equilibrium configuration for the chiral nematic deformation profile is such that the total free energy has a minimal value subject to the boundary conditions. Minimization of the total free energy yields the director configuration. The total free energy density of the chiral nematic slab is calculated using Eqs. (3- 10):

$$\begin{aligned} f_{el} + f_{chiral} + f_{field} = & \frac{1}{2} (k_{11} \cos^2 \theta + k_{11} \sin^2 \theta) \theta^{(1)2} + \\ & \frac{1}{2} \cos^2 \theta (k_{22} \cos^2 \theta + k_{33} \sin^2 \theta) \varphi^{(1)2} - \\ & k_{22} \frac{2\pi}{p} \cos^2 \theta \varphi^{(1)} + \frac{1}{2} k_{22} \left(\frac{2\pi}{p}\right)^2 - \frac{1}{2} \mu_0^{-1} x_{\alpha} B^2 \sin^2 \theta \end{aligned} \quad (11)$$

where  $\theta^{(1)} = \partial \theta / \partial z$  and  $\varphi^{(1)} = \partial \varphi / \partial z$ . Using the Euler-Lagrange approach to minimize the free energy leads to

$$\begin{aligned} g(\theta) \theta^{(2)} + \frac{1}{2} g(\theta) \theta^{(1)2} - \frac{1}{2} h(\theta) \varphi^{(1)2} - \\ 2k_{22} \left(\frac{2\pi}{p}\right) (\sin \theta \cos \theta) \varphi^{(1)} + \mu_0^{-1} x_{\alpha} B^2 \sin \theta \cos \theta = 0 \end{aligned} \quad (12)$$

$$h(\theta) \varphi^{(2)} + h'(\theta) \theta^{(1)} \varphi^{(1)} + 2k_{22} \left(\frac{2\pi}{p}\right) (\sin \theta \cos \theta) \theta^{(1)} = 0 \quad (13)$$

where  $\theta^{(2)} = \partial^2 \theta / \partial z^2$ ,  $\varphi^{(2)} = \partial^2 \varphi / \partial z^2$

$$g(\theta) = k_{11} \cos^2 \theta + k_{33} \sin^2 \theta$$

$$h(\theta) = \cos^2 \theta (k_{22} \cos^2 \theta + k_{33} \sin^2 \theta) \quad (14)$$

and the prime denotes differentiation with respect to  $\theta$ . The boundary conditions for the confined chiral nematic with weak anchoring effects at the boundary surfaces can be written as [4]:

$$\partial f_s^{1,2} / \partial \theta + \partial (f_{el} + f_{chiral} + f_{field}) / \partial \theta^{(1)} = 0 \quad (15)$$

$$\partial f_s^{1,2} / \partial \varphi + \partial (f_{el} + f_{chiral} + f_{field}) / \partial \varphi^{(1)} = 0 \quad (16)$$

Accordingly, the boundary conditions for the lower and the higher boundary surfaces, respectively at  $z = 0$  and  $z = d$ , are obtained as follows:

$$g(\theta)\theta^{(1)} \Big|_{z=0} = -W_1 (\cos \varphi \cos \theta \cos \theta_0 + \sin \theta \sin \theta_0) (\cos \varphi \sin \theta \cos \theta_0 + \cos \theta \sin \theta_0) \quad (17)$$

$$g(\theta)\theta^{(1)} \Big|_{z=d} = -W_2 (\sin \varphi \cos \theta \cos \theta_d + \sin \theta \sin \theta_d) (\sin \varphi \sin \theta \cos \theta_d + \cos \theta \sin \theta_d) \quad (18)$$

$$h(\theta)\varphi^{(1)} \Big|_{z=0} = -k_{22} \left( \frac{2\pi}{p} \right) \cos^2 \theta + W_1 (\cos \varphi \cos \theta \cos \theta_0 + \sin \theta \sin \theta_0) (\sin \varphi \cos \theta \cos \theta_0) \quad (19)$$

$$h(\theta)\varphi^{(1)} \Big|_{z=d} = -k_{22} \left( \frac{2\pi}{p} \right) \cos^2 \theta + W_2 (\sin \varphi \cos \theta \cos \theta_d + \sin \theta \sin \theta_d) (\cos \varphi \cos \theta \cos \theta_d) \quad (20)$$

Central difference discretizing scheme is used to find the director distribution as well as the dependence of the threshold field on the pitch of the chiral slab and the anchoring conditions. Specifically, a recursive method is used to solve the system of obtained equations under the boundary conditions.

## RESULTS AND DISCUSSION

For a twisted chiral nematic slab, the material parameters used in the calculation are:  $K_{33}/K_{11} = 1.25$ ,  $K_{22}/K_{11} = 0.65$  and  $\chi_a = 9.5 \times 10^{-7} (m^3 kg^{-1})$ ,  $\mu_0 = 4\pi \times 10^{-7} (Hm^{-1})$ . The director profiles for the tilt and the twist angles, under different applied fields, are calculated in the slab with weak boundary conditions. The anchoring strength is taken as  $W_{1,2} = 2 \times 10^{-4} \text{ jm}^{-2}$  for both boundary surfaces. The results are shown as functions of non-dimensional parameter  $z/d$  in Figs. 2 and 3. The results are plotted in the range of reduced magnetic fields  $B/B_{th}^0$ , in which

$B_{th}^0 = \frac{\pi}{d} \sqrt{k_{11}} / \chi_a$  is the threshold magnetic field for untwisted

nematic slab. From Fig. 2 it is clear that below the threshold field strength, the director profile is unperturbed and remains uniform. However above this value, a distortion occurs because of a competition between restoring elastic forces induced by the alignment at the boundaries, the chirality and the destabilizing torques produced by the external fields. Increasing the external field leads to reorientation of liquid crystal molecules even for molecules near the boundary surfaces due to the weak boundary conditions. The influence of the magnetic field is strongest at the middle plane of the slab, implying a balance with the maximum elastic force. The tilt angle  $\theta$  reaches the maximum  $\theta_m$ , at the mid-layer of the slab,  $\theta_m = \theta(d/2)$ . The threshold properties of the slab can be obtained through observing the behavior of  $\theta_m$ . Figure 3 shows the variation of  $\theta_m$  with respect to the different values of magnetic field and at various confinement ratios. It is found that the maximum tilt angle  $\theta_m$  increases with the ratio of  $d/P$  while the threshold field is inversely proportional to the ratio  $d/P$ . In addition, it is shown that due to the influence of chirality, higher field strengths are needed to reorient liquid crystal molecules when compared to untwisted cells [9]. Then, the threshold field, at which a phase transition occurs between unperturbed and distorted conformation is calculated. The dependence of threshold field on the confinement ratio is presented in Fig. 4. One should note that, at zero fields the texture is uniformly planar and at low field strengths, the director can be assumed to remain on average in the  $x$ - $y$  plane with the helix axis, and thus along the  $z$  axis. There is a strong competition between the surface forces trying to

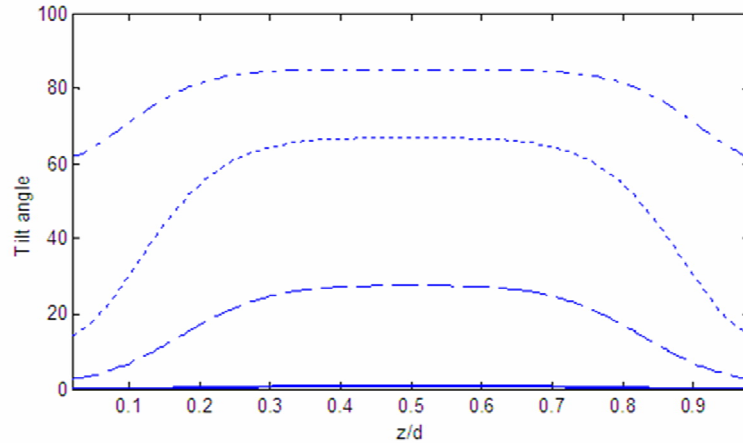


**Fig. 2.** Director profile under different applied magnetic fields for the tilt angle, in weak boundary conditions, dashed curve:  $B/B_{th}^0 = 2.4$ , dotted curve:  $B/B_{th}^0 = 4.8$ , dash-dot curve:  $B/B_{th}^0 = 6.4$ , solid curve:  $B/B_{th}^0 \ll 1$ .

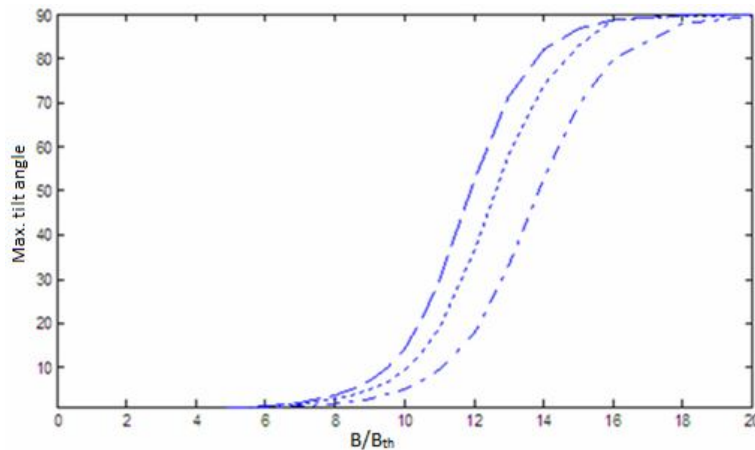


**Fig. 3.** Influence of different values of the confinement ratio,  $d/p$ , on magneto-distortional curve. Dash-dotted curve:  $d/P = 2.04$ , dotted curve:  $d/P = 3.06$ , dashed curve:  $d/P = 4.08$ .

keep the chiral nematic slab planar, *i.e.*, the helix axis perpendicular to the substrates, and the applying field trying to reorient the helix into the  $x$ - $y$  plane. This competition, depending on the relative strength of the two mechanisms, leads to different director distributions or distortions. Applying the field normal to the cholestric planar quasi-layers, the magnetic torques tend to reorient the layers along the field but free rotations are suppressed by limiting surfaces. As a result, at the weak fields, the layers undergo

some periodic director deformations [15]. The periodicity and the resultant texture strongly depend on the confinement ratio  $d/P$  [16]. The minimization of free energy favors the nematic phase if the thickness is less than the unperturbed pitch, *i.e.*, the texture does not differ much from the nematic phase. Increasing the confinement ratio leads to destabilize the planar nematic phase in the middle plane of the slab, in very strong anchoring condition.

It should be emphasized that the orientational transition

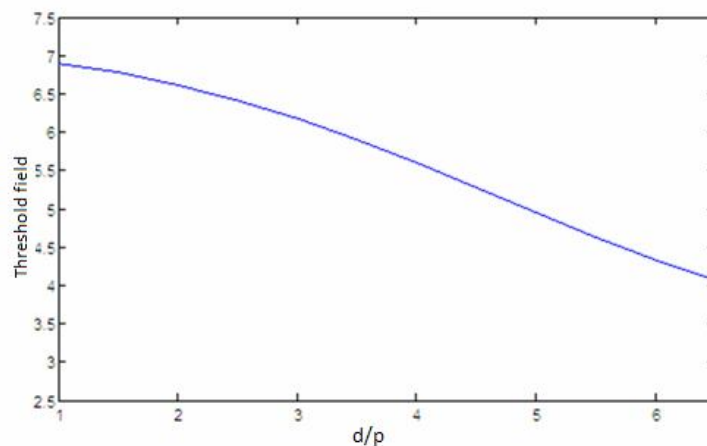


**Fig. 4.** Dependence of the threshold field on the confinement ratio,  $d/p$ , for  $W_{1,2} = 2.4 \times 10^{-4} \text{ J m}^{-2}$ .

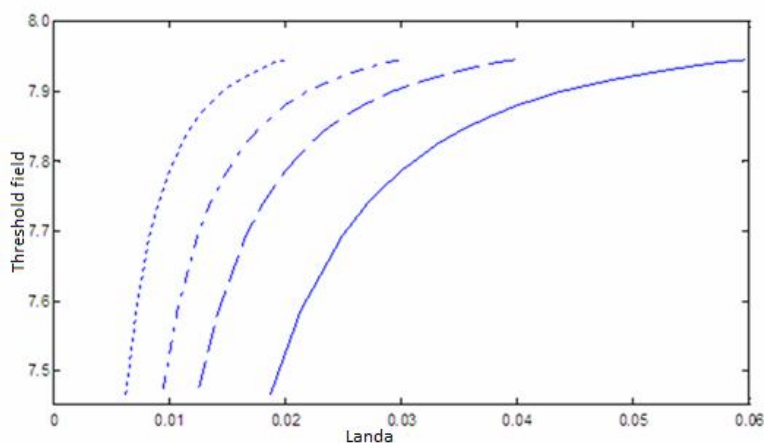


**Fig. 5.** Dependence of the threshold field on  $\lambda$ , for a twisted chiral nematic slab. Dotted curve:  $W_{1,2} = 2.4 \times 10^{-4} \text{ J m}^{-2}$ , dash-dotted curve:  $W_{1,2} = 1.6 \times 10^{-4} \text{ J m}^{-2}$ , dashed curve:  $W_{1,2} = 8 \times 10^{-4} \text{ J m}^{-2}$ , solid curve:  $W_{1,2} = 2 \times 10^{-4} \text{ J m}^{-2}$ .

happens at a fixed temperature. The confinement ratio is the parameter which characterizes the mechanical action of the two limiting surfaces and the magnetic field acts as an additional control parameter. A very strong field induces a homeotropic texture, in which the director is oriented perpendicular to the substrates and the helical axis is in the plane of the slab. The appearance of such textures, called fingerprints, depends on the confinement ratio  $d/P$  [17]. Moreover, at higher magnetic fields, helix unwinding process can happen in cases where the slab is considered thick or outside the length scale on which the surface forces are considered strong [18]. Nevertheless, this transition

is obviously different from that described above. It is expected that for these distortions, the threshold fields will not be sharp and will depend on slab dimensions, pitch length, *etc.* [4].

Meanwhile, it is convenient to introduce the dimensionless parameter  $\lambda = \pi K_{22}/W_{1,2}d$ . The dependence of the threshold field on  $\lambda$  is obtained by a similar finite difference method. The results are shown in Figs. 5 and 6. Specifically, Fig. 5 reveals that the threshold field is more sensitive to the thickness when compared to the case of weak anchoring strengths. Figure 6 shows the variation of the threshold field for different confinement ratios. It

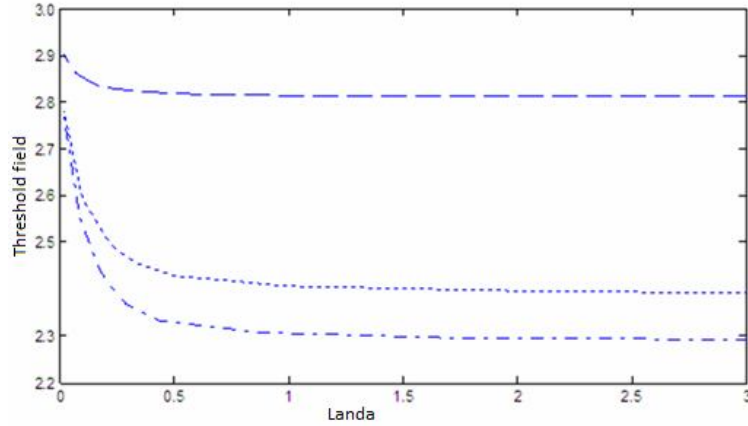


**Fig. 6.** Dependence of the threshold field on  $\lambda$ , for a twisted chiral nematic slab. Dash-dotted curve:  $d/P = 4.58$ , dotted curve:  $d/P = 4.08$ , dashed curve:  $d/P = 3.57$ .

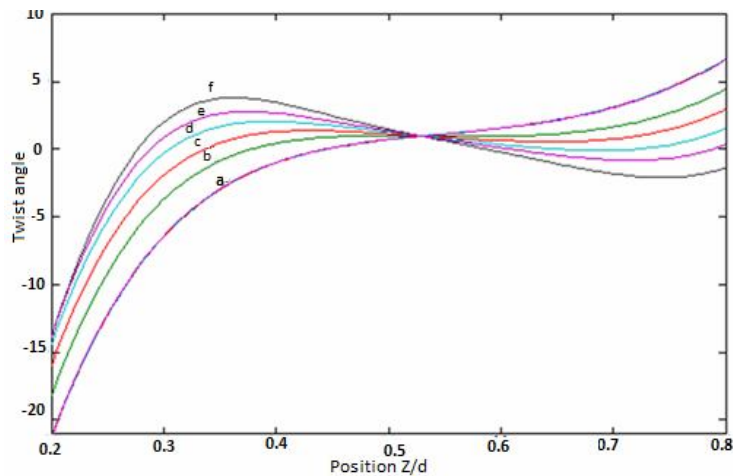


**Fig. 7.** Deformation profile in a chiral nematic slab with weak boundary conditions for the twist angle. The variation of twist angle in mid-layer is represented in the range of  $B/B_{th}^0 = 2$  to  $B/B_{th}^0 = 7$  from a to f, respectively.

confirms that for a constant ratio of  $d/P$ , the threshold field decreasing rate in strong anchoring conditions is high and that by decreasing the strength of anchoring, *i.e.*,  $\lambda > 1$ , the threshold field becomes approximately constant.

The calculated profiles for the twist angle are shown in Fig. 7. It is found that the twist angle is not symmetric with respect to the mid-layer of the slab. This is due to the asymmetric azimuthal angles of the director at the boundary planes. To find the field dependence of the twist angle, the director deformation in the mid-layers of the slab can be

determined by taking different ranges of the reduced magnetic field, as shown in Fig. 7. Another aspect of the chiral nematic response to an applied field is hysteresis. The reorientation is accompanied by hysteresis phenomena. However, it is found that the hysteresis loops disappear when the anchoring strength is sufficiently small [19].

Using our simple method which is very stable and fast can reveal some new aspects of director distribution and Fredericks transition in chiral nematic liquid crystal slabs. Also a good agreement of the solutions with the previously

reported solutions [14,20] highlights the effectiveness of this method.

## CONCLUSIONS

We discussed the director reorientation in a confined twisted chiral nematic slab and its dependence on anchoring strength, confinement ratio and magnetic field strengths. To find the effect of finite anchoring strengths, we considered the general form of surface energy. We have successfully applied an effective and stable, yet simple, method to calculate the director distribution for a twisted nematic slab. The method is based on a straightforward finite-difference approximation. We obtained the threshold fields and discussed the field dependence of the tilt and twist angles. More specifically, our process can reveal some new aspects of director deformations in complicated scenarios through a simple procedure. The Fredericks transition is important in the development of liquid crystal display devices. Hence, a detailed investigation is of significant practical relevance. Future developments can be pursued in studying dynamical features of Fredericks transition while taking into account the anchoring potentials in a chiral nematic slab [21]. Furthermore, we have not yet introduced any defects in our case. However, given the discretization, the introduction of defects in the director field, will bring about enormous technical difficulties, which will be one of the subject of our future research.

## REFERENCES

- [1] F.C. Frank, *Discuss. Faraday Soc.* 25 (1958) 19.  
W.H. De Jeu, *Physical Properties of Liquid Crystalline Materials*, Gordon and Breach Science Publishers, 1980.
- [2] P.G. De Gennes, J. Prost, *The Physics of Liquid Crystals*, Oxford, New York, 1995.
- [3] D. Demus, J. Goodby, G.W. Gray, H.W. Spiess, V. Vill, *Physical Properties of Liquid Crystals*, Wiley-VCH Verlag, Germany, 1999.
- [4] I. Dierking, *Textures of Liquid Crystals*, Wiley-VCH Verlag, 2003.
- [5] O.K. Dmitry, *Phys. Rev. E* 79 (2009) 030702/1.
- [6] E. Kadivar, K. Rahimi, M.A. Shahzamanian, *Liq. Cryst.*, 7 (2008) 815.
- [7] S. Shoarinejad, M.A. Shahzamanian, *J. Mol. Liq.* 138 (2008) 14.
- [8] G. Napoli, *J. Phys. A: Math. Gen.* 39 (2006) 11.
- [9] R.H. Self, C.P. Please, T.J. Sluckin, *Euro. J. Appl. Math.* 13 (2002) 1.
- [10] A.D. Kiselev, T.J. Sluckin, *Phys. Rev. E* 71 (2005) 031704/1.
- [11] A. Rapini, Papoular, *J. Phys. (Paris) Colloq.* 30 (1969) C4.
- [12] A. Sugimura, O.Y. Zhong, *Phys. Rev. E* 51 (1995) 784.
- [13] Y. Guochen, Z. Shu-jing, H. Li-Jun, G. Rong-Hua, *Liq. Cryst.* 8 (2004) 1093.
- [14] D. Krzyzanski, G. Derfel, *Liq. Cryst.* 951 (2002) 210.
- [15] P. Ribiere, P. Oswald, *J. Phys. (Paris)* 51 (1990) 1703.
- [16] I. Gvozdozskyy, O. Yaroshchuk, M. Serbina, *Mol. Cryst. Liq. Cryst.* 546 (2011) 202/1672.
- [17] W.C. Yipa, H.S. Kwok, *Appl. Phys. Lett.* 4 (2001) 425.
- [18] V.A. Belyakov, E.I. Kats, S.P. Palto, 1 (2004) 229.
- [19] W. Zhao, X.W. Chen, M. Iwamoto, *Phys. Rev.* 65 (2002) 031709/1.
- [20] V.A. Belyakov, *Mol. Cryst. Liq. Cryst.* 489 (2008) 54/380.